

Effect of thermal annealing of Ni/Au ohmic contact on the leakage current of GaN based light emitting diodes

Chin-Yuan Hsu, Wen-How Lan, and YewChung Sermon Wu

Citation: *Applied Physics Letters* **83**, 2447 (2003); doi: 10.1063/1.1601306

View online: <http://dx.doi.org/10.1063/1.1601306>

View Table of Contents: <http://scitation.aip.org/content/aip/journal/apl/83/12?ver=pdfcov>

Published by the [AIP Publishing](#)

Articles you may be interested in

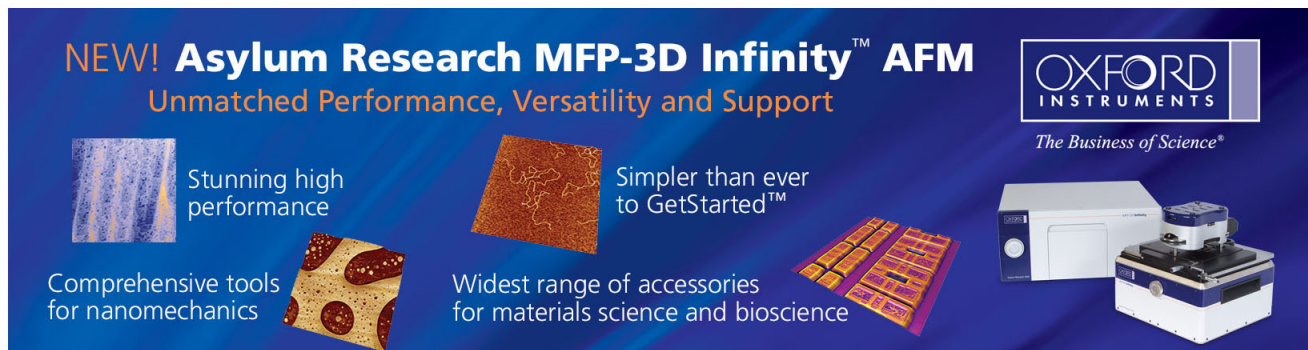
[Analysis of surface roughness in Ti/Al/Ni/Au Ohmic contact to AlGaIn/GaN high electron mobility transistors](#)
Appl. Phys. Lett. **97**, 062115 (2010); 10.1063/1.3479928

[Improved long-term thermal stability of In Ga N Ga N multiple quantum well light-emitting diodes using Ti B 2 - and Ir-based p -Ohmic contacts](#)
Appl. Phys. Lett. **90**, 242103 (2007); 10.1063/1.2748306

[Formation process of high reflective Ni Ag Au Ohmic contact for GaN flip-chip light-emitting diodes](#)
Appl. Phys. Lett. **90**, 163515 (2007); 10.1063/1.2730734

[High-reflectivity Pd Ni Al Ti Au ohmic contacts to p -type GaN for ultraviolet light-emitting diodes](#)
Appl. Phys. Lett. **85**, 2797 (2004); 10.1063/1.1805199

[Microstructural investigation of oxidized Ni/Au ohmic contact to p-type GaN](#)
J. Appl. Phys. **86**, 3826 (1999); 10.1063/1.371294




NEW! Asylum Research MFP-3D Infinity™ AFM
Unmatched Performance, Versatility and Support

OXFORD INSTRUMENTS
The Business of Science®

Stunning high performance
Simpler than ever to GetStarted™

Comprehensive tools for nanomechanics
Widest range of accessories for materials science and bioscience



Effect of thermal annealing of Ni/Au ohmic contact on the leakage current of GaN based light emitting diodes

Chin-Yuan Hsu

Department of Materials Science and Engineering, National Chiao Tung University, Hsinchu 300, Taiwan, Republic of China

Wen-How Lan^{a)}

Department of Electrical Engineering, National University of Kaohsiung, Kaohsiung 811, Taiwan, Republic of China

YewChung Sermon Wu

Department of Materials Science and Engineering, National Chiao Tung University, Hsinchu 300, Taiwan, Republic of China

(Received 3 December 2002; accepted 16 June 2003)

The effect of thermal annealing on current–voltage properties of GaN light emitting diodes (LEDs) has been studied. At annealing temperatures above 700 °C, the *p*–*n* junction of the diodes became very leaky and Ga-contained metallic bubbles were observed on the surface of Ni/Au *p*-ohmic contact. Transmission electron microscopy and energy dispersive x-ray spectrometer studies revealed that these metallic bubbles resided directly on top of the threading dislocations in GaN and both Ni and Au were indiffused into the LED structure along the cores of the TDs. The conducting paths formed by the metal containing dislocation cores are believed to be the cause for the observed short circuit behavior of *p*–*n* junctions at high annealing temperatures. © 2003 American Institute of Physics. [DOI: 10.1063/1.1601306]

GaN-based light emitting diodes (LEDs) operating in the green to violet range of the visible spectrum is commercially available and got a great interest these years. In the device process step, a good ohmic contact is necessary to achieve a high performance device. Also, the thermal stability of these contacts is an important issue for device operation.

In the fabrication of ohmic contact to GaN, different metals were applied in both *n* and *p* type. For *n*-type GaN, low resistance ohmic contacts around 10^{-5} – 10^{-8} Ω cm² range have been obtained using Ti/Al metals series.^{1–3} For *p*-type GaN, the high work function metals such as Ni, Pd, and Pt were applied. The specific contact resistance around 10^{-2} – 10^{-6} Ω cm² can be achieved in the Ni/Au, Pd/Au, Ni/Pt/Au, Pd/Pt/Au, and Ni/Pd/Au series.^{4–7} The annealing process around 400–750 °C is necessary to achieve good ohmic properties for both *n*- and *p*-type case. However, the heat generated by the ohmic loss in the device operation is an important reason to cause the device degradation.⁸ The serious degradation in contact morphology can also be observed at higher temperature process due to the formation of new interfacial phases.^{9,10}

Some literatures reported that the threading dislocation (TD) may degrade the device performance and is a nonradiative recombination center in GaN.^{11,12} The TD provided a diffusion pathway of metals and cause the leakage current in GaN-based devices.^{13–15} It is also an important source of reverse leakage current in diodes and cause the poor electrostatic discharge behavior in the devices.^{16–18}

Thus, we know both contact metals and TDs affect the *I*–*V* characteristics of the GaN-based devices. Yet, lack of

direct studies about the electric properties of the contact metals and TDs. In this work, we fabricate the GaN-based multiquantum well (MQW) structure LEDs and study the electric properties under different thermal treatment. The surface morphology and microstructure of these LEDs with different thermal treatment have been characterized by scanning electron microscopy (SEM) and transmission electron microscopy (TEM) analysis. Compare with the electrical properties, the existence and influences of dislocations on LEDs can be clearly characterized in this work.

The blue GaN-based MQW LEDs wafers were grown by metalorganic chemical vapor deposition on *c*-plane sapphire substrate. Trimethylgallium, trimethylindium, and ammonia were used as Ga, In, and N precursors, respectively. The layer structure consists of a GaN buffer layer, followed by a 1.5 μ m undoped GaN layer, a 3 μ m Si-*(n)* doped GaN layer

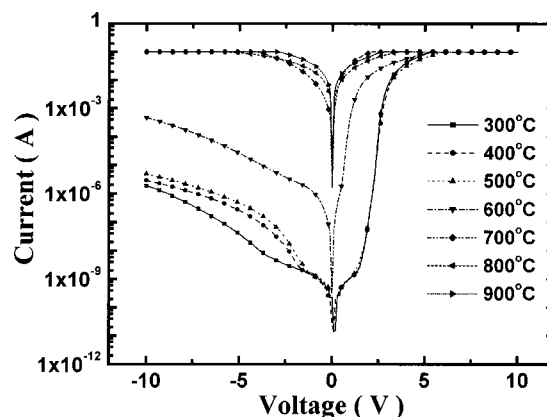


FIG. 1. *I*–*V* characteristics of GaN LEDs at various annealing temperatures.

^{a)}Electronic mail: whlan@nuk.edu.tw

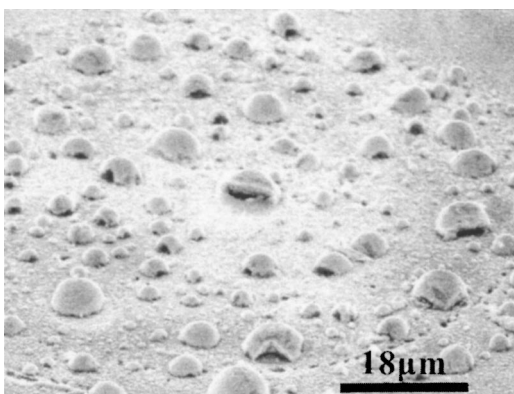


FIG. 2. SEM image of Ni/Au on *p*-GaN contact surface after annealing at 900 °C.

($n \sim 1 \times 10^{18} \text{ cm}^{-3}$), the active layer, a 0.12- μm -thick Mg-(*p*) doped AlGaIn cladding layer ($p \sim 5 \times 10^{17} \text{ cm}^{-3}$), and a Mg-(*p*) doped GaN contact layer ($p \sim 7 \times 10^{17} \text{ cm}^{-3}$). The active region, consisting of seven 5 nm/15 nm InGaIn/GaN quantum wells is embedded in the region between *p*-type and *n*-type layers.

The LEDs are fabricated using standard lithography. In the first process step, a mesa is defined with standard photolithography and etched down into the *n*-type region by inductively coupled plasma reactive ion etching technology. The thin Ni/Au (5 nm/5 nm) transparent contact layer (TCL) was deposited by electron (e)-beam evaporation and defined

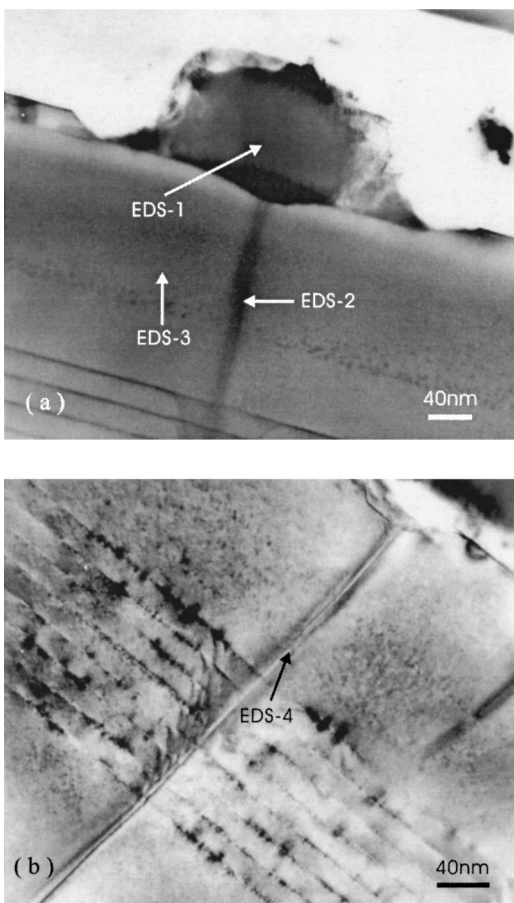


FIG. 3. Cross-section bright-field TEM micrographs of the LEDs structure after annealing at (a) 900 and (b) 600 °C.

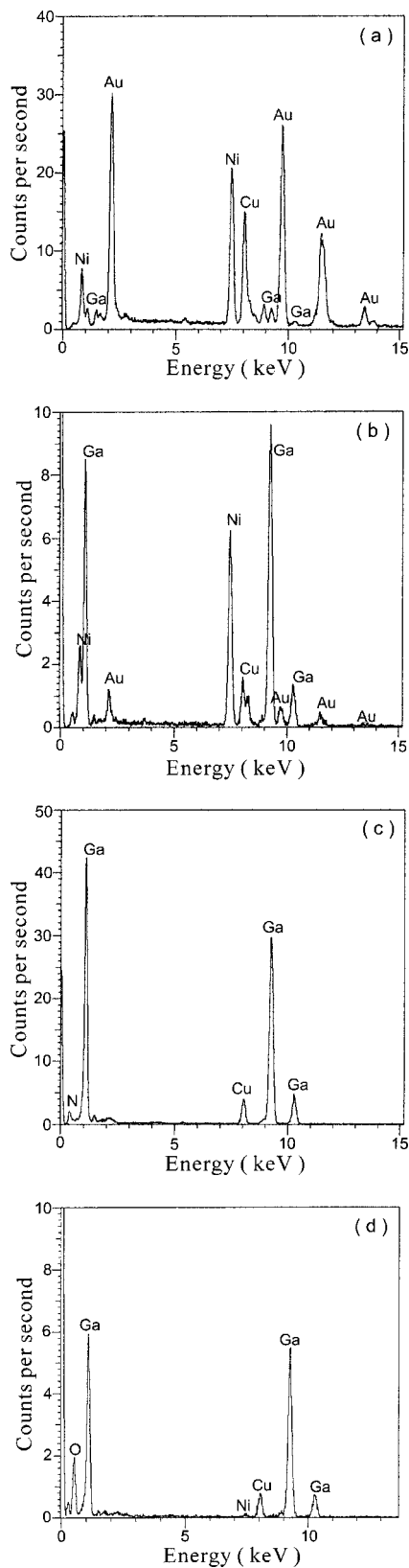


FIG. 4. EDS spectra obtained from different regions: (a) EDS-1 at metallic bubble of Fig. 3(a), (b) EDS-2 at threading dislocation of Fig. 3(a), (c) EDS-3 at *p*-GaN layer of Fig. 3(a), and (d) EDS-4 at threading dislocation of Fig. 3(b).

on the *p*-GaN region. A thick Ni/Au (50 nm/150 nm) contact layer was fabricated on the thin Ni/Au TCL with standard lift-off technology by the same e-beam evaporation, followed by a 500 °C annealing process. The Ti/Al/Ti/Au (10 nm/50

nm/100 nm/150 nm) metals for the *n* contact are then deposited on the *n*-GaN layer, followed by the annealing process at 300 °C.

The wafers were then cut into chips. These chips were then annealed with different temperatures in a furnace with continuous nitrogen flow in ten minutes. The electrical characteristics were measured at room temperature with HP-4155 *I*-*V* analyzer. For TEM measurements, the specimens were carried out by JEOL JEM-2010 microscope operated at 200 kV. The SEM surface images were taken with Hitachi S-4000 instrument.

Figure 1 shows the *I*-*V* characteristic of GaN based LEDs with different annealing temperatures. In the forward bias region, similar *I*-*V* characteristics with the ideal factor around 2.9 can be seen with annealing temperature below 500 °C. Thus, the similar electron-hole recombination behavior can be expected in this region. The reverse bias current increase a little as the anneal temperature increase from 300 to 500 °C. A small leakage path may be formed in the range and may increase as the temperature increase. Yet, there is no obvious surface morphology change on these chips.

While the annealing temperature higher than 700 °C, the electrical short circuit behavior can be observed and the LEDs become lightless. The short circuit resistance decreases as the annealing temperature increases. Thus, a main leakage path can be expected and increase as the annealing temperature increase from 700 to 900 °C.

Figure 2 shows the SEM image of thick Ni/Au contact layer on *p*-GaN surface after 900 °C annealing process. A lot of bubbles with diameter around submicrometer to 10 μm can be observed. These bubbles cause the surface morphology change and can be observed on the chips with the annealing temperature higher than 600 °C. These bubbles may be formed from the sintering of Ni/Au to *p*-GaN and degrade the properties of the LEDs.

Figure 3(a) shows the TEM cross-sectional image after annealing at 900 °C. A hollow center of the bubble can be seen clearly in this figure. Below the metallic bubble, the straight TD can be found on (1 $\bar{1}$ 00) plane. In Fig. 3(b), the straight TD can be also observed after annealing at 600 °C. Using the energy dispersive x-ray spectrometer (EDS), the compositions were analyzed. There are four interesting regions: the metallic bubble (EDS-1), the TD (EDS-2), the *p*-GaN layer (EDS-3) of Fig. 3(a), and the TD (EDS-4) of Fig. 3(b). Figure 4 shows the EDS spectra of these regions. In the EDS-1, the main compositions are Ni, Ga, and Au as shown in Fig. 4(a). After the EDS spectrum analysis, the phases were characterized as the Ga-containing compounds, such as Ga₄Ni₃, Ga₃Ni₂, GaAu, and GaAu₂.¹⁷ These phases may be formed due to the Ga outdiffusion in the annealing process. The metallic bubbles may be formed from the gasification of the nitrogen with the decomposition of GaN.

The EDS spectrum of the EDS-2 was shown in Fig. 4(b). Compared to the EDS spectrum of the EDS-3 as shown in Fig. 4(c), the Ni and Au can be observed clearly in the TD region after annealing at higher temperature. Compared to

the surface morphology as shown in Fig. 2, the Ni and Au may migrate on top of the TDs and indiffuse along the TDs in the annealing process. The indiffusion process can only occurred with the TDs since there are no Ni and Au signals with *p*-GaN region as shown in Fig. 4(c). The diffusion of Ni and Au along the TD through the MQW structure may cause a short circuit current path from *p*-GaN to *n*-GaN region. Furthermore, the TD region only contains very small amount of Ni signal after annealing at 600 °C as shown in Fig. 4(d). Thus, the short circuit behavior as shown in Fig. 1 with annealing temperature higher than 600 °C can be realized. Our studies provide the direct evidence that metals indiffusion along the TDs cause the degradation of the LEDs characteristics.

In conclusion, the influences of thermal annealing on electrical properties of GaN LEDs have been investigated. After annealing above 700 °C, the electrical short circuit behavior has been observed. At annealing 900 °C, Ga-contained metallic bubbles have been observed on the *p*-GaN surface by SEM. Both TEM and EDS analyses reveal that the core of the TD contains Ni and Au after annealing higher temperatures. These results imply direct evidences that the migration and indiffusion of Ni and Au along the TDs cause the short circuit characteristics of the *p*-*n* junction at high temperatures.

This work was partially supported by Formosa Epitaxy Incorporation, Taiwan, Republic of China.

- ¹J. S. Foresi and T. D. Moustakas, Appl. Phys. Lett. **62**, 2859 (1993).
- ²M. E. Lin, Z. Ma, F. Y. Huang, Z. F. Fan, L. H. Allen, and H. Morkoc, Appl. Phys. Lett. **64**, 1003 (1994).
- ³Z. Fan, S. Mohammad, and W. Kim, Appl. Phys. Lett. **68**, 1672 (1996).
- ⁴J. K. Ho, C. S. Jong, C. C. Chiu, C. N. Huang, and K. K. Shih, Appl. Phys. Lett. **74**, 1275 (1999).
- ⁵J. K. Kim, J. L. Lee, J. W. Lee, H. E. Shin, Y. J. Park, and T. Kim, Appl. Phys. Lett. **73**, 2953 (1998).
- ⁶J. S. Jang, K. H. Park, H. K. Jang, H. G. Kim, and S. J. Park, J. Vac. Sci. Technol. B **16**, 3105 (1998).
- ⁷C. F. Chu, C. C. Yu, Y. K. Wang, J. Y. Tsai, F. I. Lai, and S. C. Wang, Appl. Phys. Lett. **77**, 3423 (2000).
- ⁸S. Nakamura, M. Senoh, and T. Mukai, Appl. Phys. Lett. **62**, 2390 (1993).
- ⁹Q. Z. Liu and S. S. Lau, Solid-State Electron. **42**, 677 (1998).
- ¹⁰M. E. Lin, Z. Ma, F. Y. Huang, Z. F. Fan, L. H. Allen, and H. Morkoc, Appl. Phys. Lett. **64**, 1003 (1994).
- ¹¹S. J. Rosner, E. C. Carr, M. J. Ludowise, G. Girolami, and H. I. Erikson, Appl. Phys. Lett. **70**, 420 (1997).
- ¹²T. Sugahara, H. Sato, M. Hao, Y. Naoi, S. Kurai, S. Tottori, K. Yamashita, K. Nishino, L. T. Romano, and S. Sakai, Jpn. J. Appl. Phys., Part 2 **37**, L398 (1998).
- ¹³C. Sasaoka, H. Sunakawa, A. Kimura, M. Nido, and A. Usui, J. Cryst. Growth **189/190**, 61 (1998).
- ¹⁴A. Osinsky, S. Gangopadhyay, R. Gaska, B. Williams, M. A. Khan, D. Kuksenkov, and H. Temkin, Appl. Phys. Lett. **71**, 2334 (1997).
- ¹⁵S. Nakamura, J. Cryst. Growth **201/202**, 290 (1999).
- ¹⁶P. Kozodoy, J. P. Ibbetson, H. Marchand, P. T. Fini, S. Keller, J. S. Speck, S. P. DenBaars, and U. K. Mishra, Appl. Phys. Lett. **73**, 975 (1998).
- ¹⁷J. K. Sheu, Y. K. Su, G. C. Chi, W. C. Chen, C. Y. Chen, C. N. Huang, J. M. Hong, Y. C. Yu, C. W. Wang, and E. K. Lin, J. Appl. Phys. **83**, 3172 (1998).
- ¹⁸J. W. P. Hsu, M. J. Manfra, D. V. Lang, S. Richter, S. N. G. Chu, A. M. Sergent, R. N. Kleiman, L. N. Pfeiffer, and R. J. Molnar, Appl. Phys. Lett. **78**, 1685 (2001).